

Prospects for dynamically formed Binary BHs from GCs in the Local Universe

Dongming Jin¹, Matthew Benacquista^{1,2}

¹Dept. of Physics, University of Texas at Arlington
²Dept. of Physics, University of Texas Rio Grande Valley
 Contact: dongming.jin@mavs.uta.edu

Abstract

The dynamical evolution of globular clusters is expected to produce stellar mass binary black holes with higher total mass than found in the field population of binary black holes. We use the Monte Carlo code MOCCA^[1] to simulate the production of binary black holes from globular clusters. These compact binary systems are found to be ejected quickly from the host globular cluster. Thereafter, they evolve independently in the form of gravitational radiation. We model the population of globular cluster out to 30 Mpc. We discuss here the prospects for detecting dynamically formed binary black holes at extragalactic distances using space-borne gravitational wave detectors.

How many GCs in each Galaxy?

To estimate the population of GCs, we used the Harris extragalactic catalog^[2] to estimate the correlation between S_N and the host galaxy. Using Random Forest importance ranking, the K-band magnitude is found to be more significantly correlated, as observational data is short on dynamical mass and other aspects.

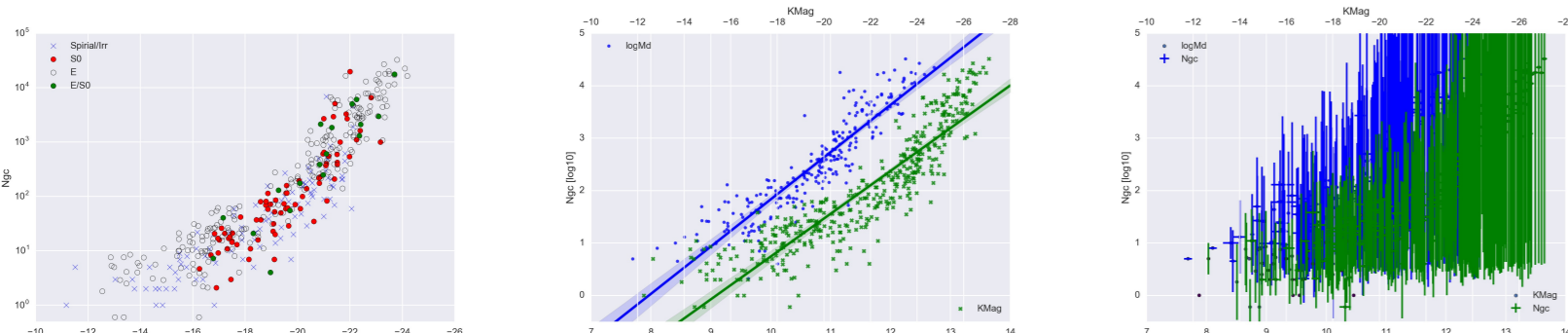


Figure 1: Best linear fit model and its problems when error is considered.

GC S_N model (Fig 2) improves on the linear model, by suppressing the error in the high-L end. Morphological type has been studied but cannot be well-modeled at this stage.



Figure 2: GC S_N is number of clusters per unit galaxy luminosity.

Due to limited extragalactic GC information, the GC age is estimated based on the age spread of 55 MWGC^[2]. The scale is a demonstration of the parameters in this study. The GC S_N model is then applied on GWGC catalog to estimate the GCs.

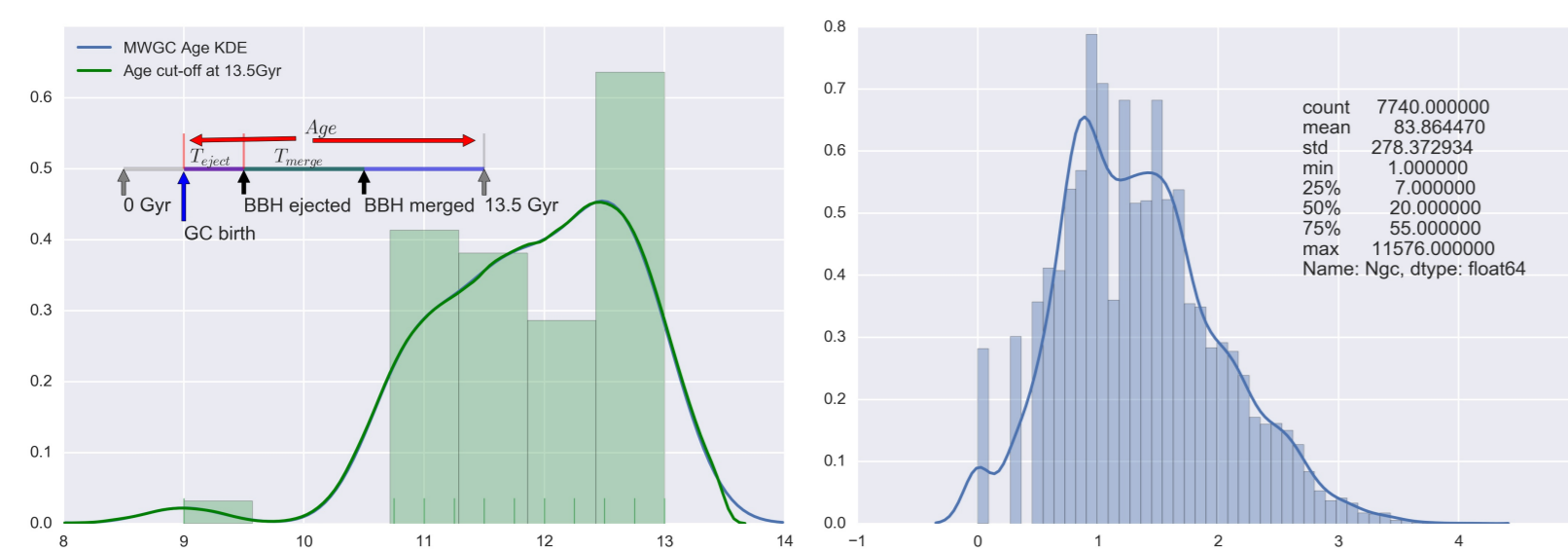


Figure 3: Hubble time is used as cut-off of the age spread. 649111 GCs are found within 30 Mpc.

What kind of GCs?

To characterize the GCs in the local universe, We adapt parameters from Table 2 to span the diversity of luminosity, metallicity and concentration from observation. The general setup is taken from the million body simulation^[3,4]. 2592 simulations are conducted with MOCCA using the TACC cluster. These models are then randomly matched to GCs.

Table 1: General setup

| | |
|--------------------------|----------------|
| Model | King $W_0 = 6$ |
| M_{\max} | $100M_{\odot}$ |
| IMF | Kroupa 1993 |
| Binary a_{semi} | Kroupa 2013 |
| a_{\max} | 50 AU |
| ecc | Thermal |
| Interaction | Fewbody |

Table 2: Parameter space

| | |
|--------------------|-----------------------|
| N | [0.5M, 1M] |
| [Fe/H] | [-1.54, -0.56, solar] |
| f_b | [0:0.1:0.5] |
| R_{tidal} | [25, 50, 100] |
| R_{plum} | [20, 25, 60] |
| Repeat | 8 |
| Total | 324 x 8 |

All sky distribution of galaxies

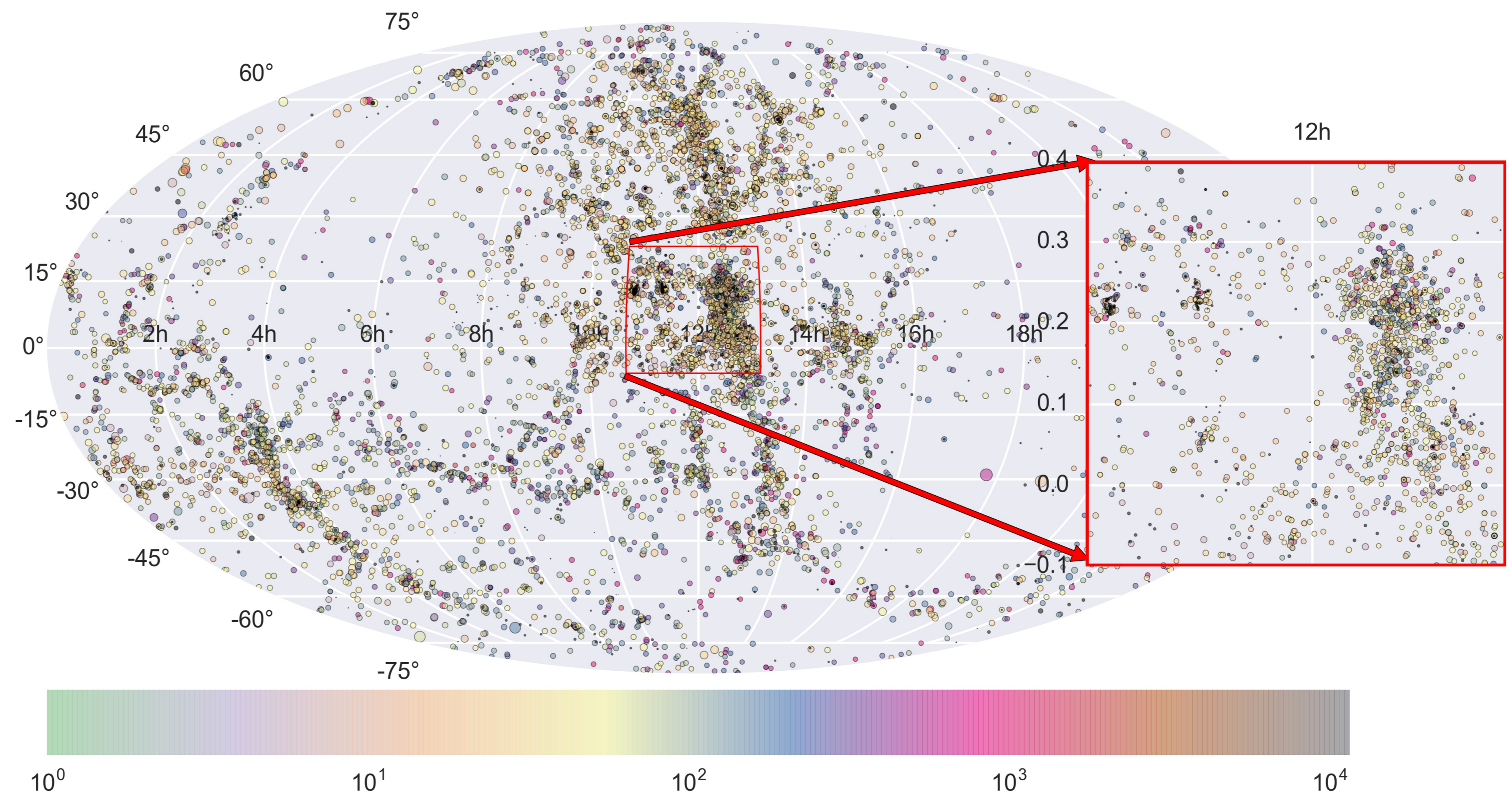


Figure 4: Mollweide projection of galaxy distribution. The color indicates the number of GCs hosted. Bigger circles indicates closer distance of the galaxy.

Dynamically formed BBHs from GCs

GCs produce large numbers of BBHs within the core and eject them by energetic dynamical encounters. These ejected BBHs undergo orbital evolution mostly by gravitational radiation. The separation and eccentricity change by the following equations.

$$\left\langle \frac{da}{dt} \right\rangle = -\frac{64G^3 m_1 m_2 (m_1 + m_2)}{5 c^5 a^3 (1 - e^2)^{7/2}} \left(1 + \frac{73}{24} e^2 + \frac{37}{96} e^4 \right) \quad (1)$$

$$\left\langle \frac{de}{dt} \right\rangle = -\frac{304G^3 m_1 m_2 (m_1 + m_2)}{15 c^5 a^4 (1 - e^2)^{5/2}} \left(1 + \frac{121}{304} e^2 \right) \quad (2)$$

Event rate of BBH mergers

Stellar mass BBH merger signals can be detected out to redshift $z \simeq 0.6$, or $d_c \simeq 2.206$ Gpc. $\mathcal{R}(d_c)$ is defined as the merger event density, which counts for the event rate at unit comoving volume per year^[4].

$$\mathcal{R}(d_c) = f \langle N_{GC} \rangle, P_{NGC}, P_{Galaxy}(d_c) \quad (3)$$

where $\langle N_{GC} \rangle$ is average merger amount per GC model, P_{NGC} is GCs population per Galaxy, $P_{Galaxy}(d_c)$ is spatial distribution of GW galaxies. The numerical integration gives an event rate: $\eta = 0.01317 \text{ Gpc}^{-3} \text{ yr}^{-1}$.

Present BBHs & frequency evolution

The binary frequency evolves in the following manner:

$$\dot{f} = k_0 f^{11/3} \quad k_0 = \frac{96}{5} (2\pi)^{8/3} \frac{G^{5/3}}{c^5} M_{\text{chirp}}^{5/3} \quad (4)$$

Assuming $N = \int dn = \int \eta dt$, we have:

$$dn = \eta dt = \frac{\eta}{k_0} f^{-11/3} df \quad (5)$$

A quick analysis can be drawn for $f_{\min} = 10^{-4.0}$ Hz. Table 3 lists 7 BBHs under this criteria, which gives a lower bound of $\eta = 0.03223 \text{ Gpc}^{-3} \text{ yr}^{-1}$.

This study doesn't count the BBH merger events that occur before the ejection. There are other dynamical formation channels in AGN, UDG which can supplement the merge event rate for ground-based gravitational wave detectors. The result suggests that dynamically formed BBH inspirals are promising sources for space-borne gravitational wave detectors.

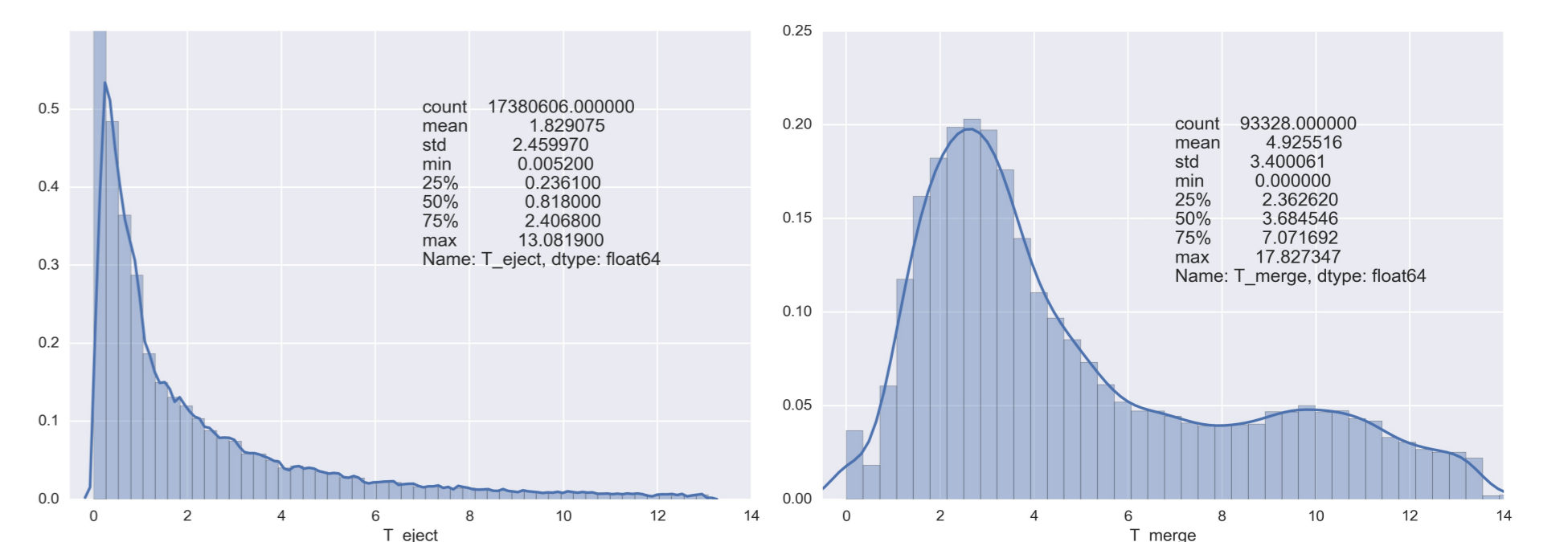


Figure 5: Most BBHs are ejected in the early stage of GC evolution. The bimodal feature of merger times is due to the chosen bimodal GC age spread.

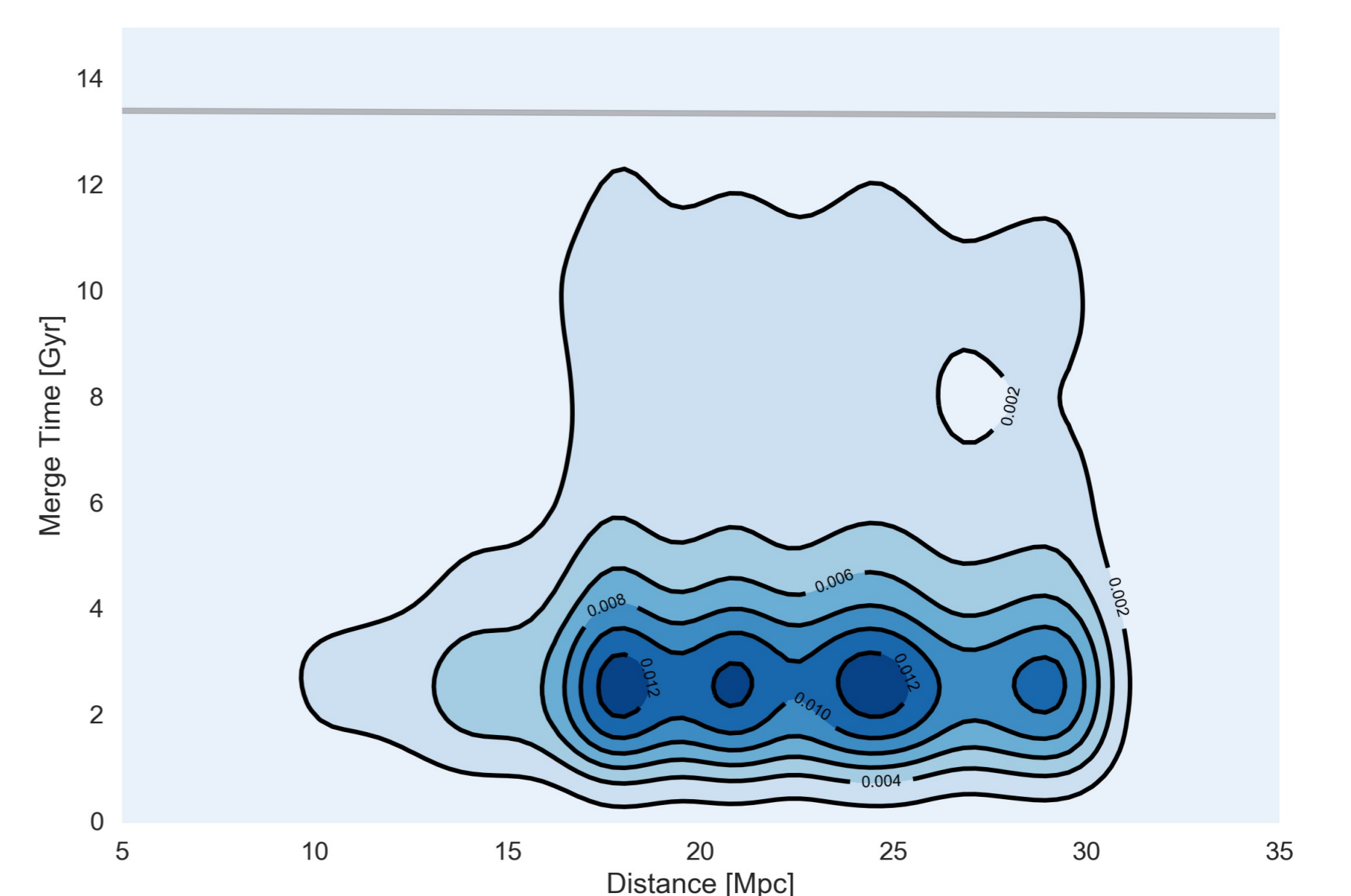


Figure 6: KDE of merger sources versus distance. The gray line is the 1 year integration of the merge event density over comoving distance, up to 30 Mpc.

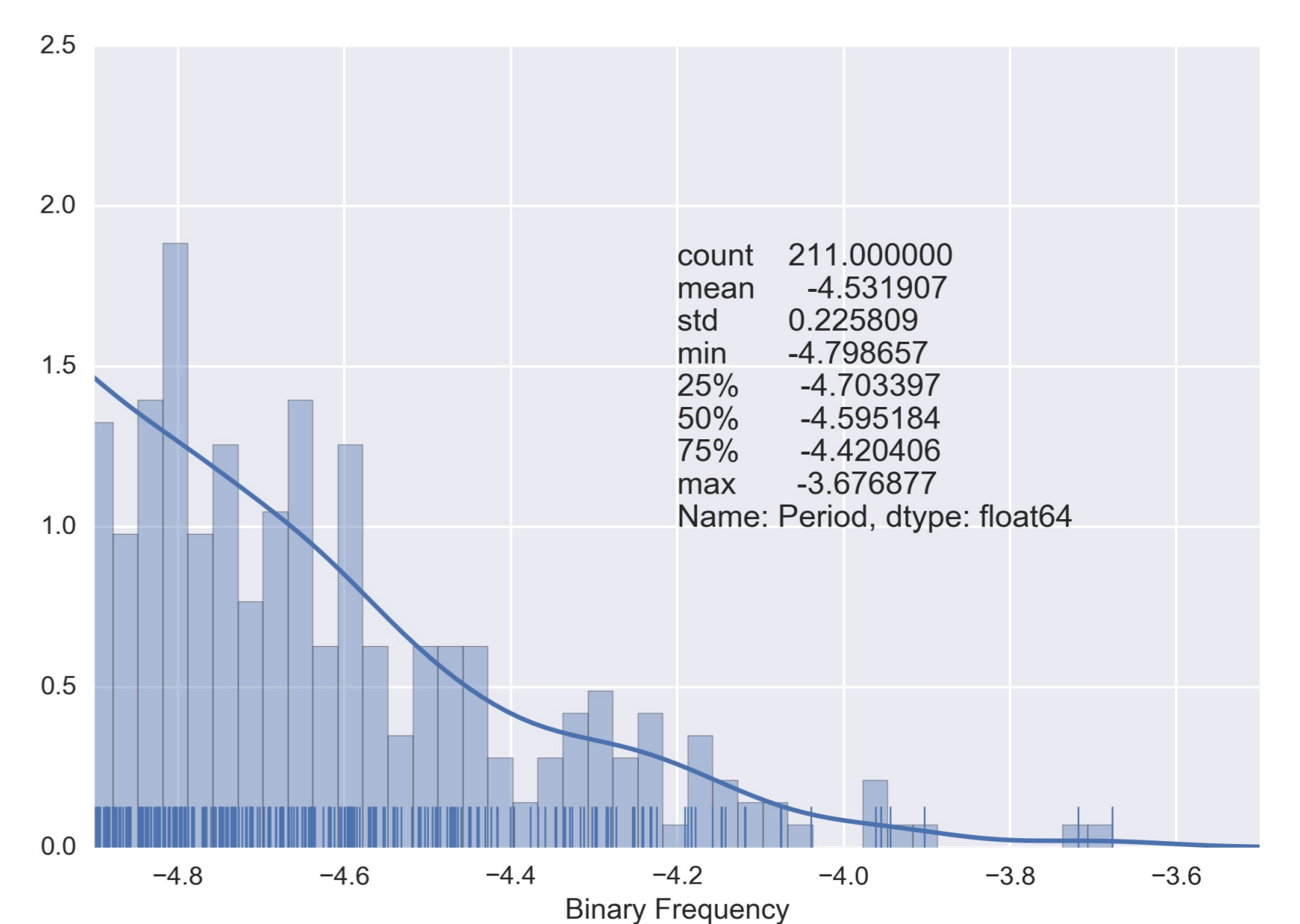


Figure 7: The binary frequency is logarithmic.

Table 3: BBHs with frequency higher than $10^{-4.0}$ Hz

| RA | Dec | Dist | Model | Age | T_{eject} | M_1 | M_2 | M_{chirp} | a | e | Period |
|--------|---------|--------|-------|--------|--------------------|--------|--------|--------------------|-------|-------|-----------|
| 23.017 | 30.145 | 13.243 | 82-5 | 11.391 | 0.354 | 25.812 | 51.586 | 31.395 | 0.029 | 0.137 | 17564.449 |
| 3.641 | -35.451 | 19.953 | 268-3 | 11.308 | 6.294 | 13.569 | 13.439 | 11.756 | 0.021 | 0.332 | 18027.777 |
| 12.514 | 12.391 | 17.219 | 287-2 | 11.732 | 1.747 | 15.263 | 63.075 | 25.781 | 0.029 | 0.262 | 18041.904 |
| 22.131 | 31.359 | 14.997 | 242-5 | 12.531 | 10.379 | 19.155 | 26.336 | 19.504 | 0.016 | 0.318 | 9504.009 |
| 7.451 | 80.178 | 28.973 | 181-2 | 10.564 | 2.994 | 47.715 | 12.773 | 20.636 | 0.019 | 0.146 | 10457.932 |
| 12.032 | -18.886 | 20.797 | 203-1 | 11.877 | 1.509 | 25.001 | 13.354 | 15.753 | 0.023 | 0.283 | 18310.303 |
| 12.365 | 4.474 | 18.030 | 203-1 | 11.879 | 1.509 | 25.001 | 13.354 | 15.753 | 0.021 | 0.253 | 16001.340 |

Reference

- [1]: M. Giersz, 1998, 2001, 2006
- [2]: W. E. Harries, et al, 2013, 2015
- [3]: L. Wang, et al, 2015
- [4]: C. Rodriguez, et al, 2016